Aeroelastic optimization of composite wings including fatigue loading requirements

Rajpal, D.; Kassapoglou, C.; De Breuker, R.

DOI
10.1016/j.compstruct.2019.111248

Publication date
2019

Document Version
Accepted author manuscript

Published in
Composite Structures

Citation (APA)
Rajpal, D., Kassapoglou, C., & De Breuker, R. (2019). Aeroelastic optimization of composite wings including fatigue loading requirements. *Composite Structures*, *227*, Article 111248. https://doi.org/10.1016/j.compstruct.2019.111248

Aeroelastic optimization of composite wings including fatigue loading requirements☆

D. Rajpal[a,*], C. Kassapoglou[a], R. De Breuker[a]

[a]*Department of Aerospace Structures and Computational Mechanics, Faculty of Aerospace Engineering, Delft University of Technology*

Abstract

An analytical model to predict the fatigue life of a composite laminate is formulated. The model calculates stresses in each ply using classical lamination theory, degrades the residual strength using the linear wear-out law and predicts failure based on Tsai Wu failure theory. The cycles to failure are predicted using the updated cycle-by-cycle probability of failure. The predictions are validated for both a constant amplitude and a variable amplitude loading on a Glass/Epoxy laminate. Additionally the analytical model is extended to work with laminates described using lamination parameters instead of ply angles and stacking sequence. The analytical fatigue model is then integrated in the TU Delft aeroelastic and structural optimization tool PROTEUS. A thickness and stiffness optimization of the NASA Common Research Model (CRM) wing has been carried out. Results show that fatigue, strength and stiffness are the design drivers in the aeroelastic optimization of a composite wing. Furthermore, by including the analytical fatigue model instead of using a traditional knockdown factor to account for fatigue, a lighter wing is obtained.

Keywords: Aeroelasticity, Structural Optimization, Fatigue, Composite Wing

1. Introduction

Structural weight reduction is one of the key approaches to reduce the fuel consumption and hence increase the performance of an aircraft. With high specific strength, the use of composite materials can be beneficial in terms of weight saving. A further advantage of the composite materials is their inherent anisotropic behavior, which can be tailored to achieve beneficial aeroelastic deformations and hence improved performance during the flight, thus providing a higher efficiency with a minimum weight penalty.

☆Part of this work has been presented in Rajpal, D., Kassapoglou, C., and De Breuker, R. Aeroelastic optimization of composite wings subjected to fatigue loads. In 2018 AIAA/ASCE/AHS/ASC Structures, Structural Dynamics, and Materials Conference.

*Corresponding author.
Address: Kluyverweg 1, 2629 HS Delft, The Netherlands.
Email address: d.rajpal@tudelft.nl

In a majority of the studies [1] dealing with the aeroelastic tailoring of the composite wings, the main design drivers are stiffness, static strength, buckling and static and dynamic aeroelastic stability. In order to avoid fatigue problems, a conservative knockdown factor is applied to the allowable material strain levels. With this design philosophy, failure under repeated loading is avoided since the fatigue loads acting on the structure are too low to initiate or propagate any existing damage. As composite wing designs become more optimized for improved aeroelastic behavior and further weight savings, the difference between the magnitude of typical fatigue loads and ultimate static strength of a design becomes smaller. As a result, fatigue loading which, historically, was not a design driver for the composite structure, now becomes more important and may impact the design. This means that using conservative knock-down factors would be too conservative and weight-inefficient. There is, therefore, a need for a fatigue analysis approach which is sufficiently accurate and efficient so it can be used in a design and optimization framework.

Fatigue damage in composites is a complex process involving different mechanisms, such as matrix cracking, fiber breakage, delamination and fiber/matrix debonding. As a result, fatigue life prediction becomes much more complicated as compared to metals. A nice overview of the different fatigue prediction algorithms exists in the literature [2–4]. Fatigue models can be divided mostly into three categories, empirical, phenomenological and progressive damage models. Empirical models such as Miner rule [5] use the information from S-N curve or Goodman diagrams to define a damage parameter which keeps track of the fatigue life. The parameter starts with 0 and increases until the value equals 1 which indicates the final failure. Phenomenological models [6, 7] calculate the fatigue life by measuring the degradation in the macroscopic material property. This property can be the stiffness [8] or the strength [9] of the material. In the progressive damage models [10, 11], composite properties are predicted and deteriorated by modelling microscopic failures that occur on fibres, matrix and fibre/matrix interface. These models are quite complex and time consuming to run, due to the various damage mechanisms occurring in composites and the extensive simulations needed to track damage evolution.

For the current study, the focus is on using residual strength phenomenological models for predicting the fatigue life of a composite. The residual strength wear out model has an inherent failure criterion: failure occurs when residual strength degrades to the maximum applied stress. There has been significant research on applying different residual strength degradation theories under a variety of loading conditions. Philippidis and Passipoularidis [9] give a nice overview of the different theories available in the literature and their validity with respect to experiments. One of the first degradation models for the residual strength which was the linear residual strength degradation approach was presented by Broutman and Sahu [12].

The approach was based on differential rate type equation which was also used in models by Schaff and Davidson [13, 14], Hahn and Kim [15] and Hashin [16]. Chou and Croman [17] and Yang along with his colleagues [18–21] used a similar type of rate equation along with probability distribution of static strength, fatigue life and residual strength. Several other authors also worked on residual strength degradation model such as Adam et al. [22], Epaarachchi and Clausen [23] and Reifsnider and Stinchcomb [24]. The majority of the models requires empirical parameters that are determined by using experiments and curve-fitting. This makes the universal application of fatigue models quite difficult. Based on the models developed by Broutman and Sahu [12], Kassapoglou [25–27] formulated a residual strength wear out model without the need of parameters obtained from fatigue tests.

In the present study, an analytical model based on the Kassapoglou method has been formulated to determine the fatigue life of a composite laminate. The model is validated for a constant amplitude as well as a variable amplitude fatigue test by comparing the prediction on a Glass/Epoxy laminate subjected to Wisper spectrum [28] and New Wisper spectrum [29]. The experimental data of the Glass/Epoxy laminate is obtained from the OPTIMAT blades database [30]. This database includes a large enough number of specimens which gives accurate values of the experimental scatter which is a variable needed as an input in the method by Kassapoglou. To integrate into an aeroelastic optimization framework, the analytical fatigue model is modified to work with the composite laminates described by lamination parameters instead of stacking sequence and ply angles. Furthermore, aeroelastic tailoring of the NASA CRM [31] wing is carried out to investigate the effect of including fatigue as one of the design constraints along with strength, buckling and aeroelastic stability.

The innovations of this paper can be summarized as follows:

- The analytical fatigue model based on the Kassapoglou method [25–27] that does not require any curve-fitting parameters has been formulated for both constant amplitude as well as spectrum loading. The model can be used to predict fatigue lives for composite laminates described in terms of both stacking sequence and lamination parameters.

- An aeroelastic optimization of a composite wing which includes fatigue as a constraint is performed. The results show that a composite tailored wing is driven not only by strength and buckling but also by fatigue.

2. Fatigue Model

The analytical fatigue model combines the Kassapoglou method [25–27, 32] with the first ply failure theory to determine the fatigue life under a constant amplitude as well as a spectrum loading.

2.1. Kassapoglou Method

For the sake of completeness, the relevant steps involved in assessing the fatigue life using the Kassapoglou method are summarized below.

1. For the given loads, stresses in each ply of the laminate can be determined using the classical laminate theory.
2. Based on the applied stress σ, the probability p that the residual strength of the ply is not higher than the applied stress in the ply is calculated. For the 1st cycle, the residual strength σ_r is equal to the static failure strength σ_{sf}. The value of p will depend on the type of statistical distribution and stress ratio R. Generally, the static strength allowables for a composite material follow a normal distribution, two parameter Weibull or lognormal distribution [32].
3. Once the probability of failure is determined, the number of cycles to failure [25], N, if the failure mode does not change and p is constant, is determined by

$$N = -\frac{1}{\ln(1-p)} \tag{1}$$

4. Residual strength of the ply after n cycles of the applied stress is determined through a degradation model [32] given by

$$\sigma_r = \sigma_{sf}(1 - (1 - \frac{\sigma}{\sigma_{sf}})\frac{n}{N-1}) \tag{2}$$

5. If the applied stress in any ply is higher than the residual strength of the ply, the laminate fails. Otherwise, the statistical parameters of the static strength, such as mean and standard deviation in case of a normal distribution are degraded and the process continues until the maximum number of cycles has been reached or the laminate has failed.

For the values of stress ratio R other than 0, the value of p, needs to be modified to account for the fact that cyclic stress doesn't start from 0 but some finite value. This is taken into account by modifying the statistical distribution of the residual strength. Figure 1 depicts the assumed change in the distribution for the stress ratio other than 0. The 1% value of the distribution is shifted towards the mean of the distribution

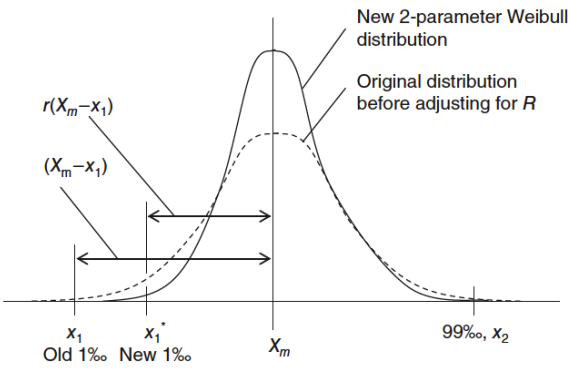

Figure 1: Modification of the probability distribution for stress ratio other than 0 [32].

by a factor r which is given by

$$\begin{aligned} r = 1 - R, 0 < R < 1 \\ r = 1 - \frac{1}{R}, R > 1 \end{aligned} \tag{3}$$

The mean and the 99 % values are kept constant. The resulting distribution is assumed to be two parameter Weibull distribution. The shape and the scale parameter can be obtained by solving iteratively the Equation (4) which is expressed as

$$\begin{aligned} \beta(1 - \frac{1}{\alpha}) = X \\ e^{-\frac{x_1^\alpha}{\beta}} - e^{-\frac{x_2^\alpha}{\beta}} = 0.98 \end{aligned} \tag{4}$$

where x_1 is the 1% value of the new distribution, x_2 is the 99 % value of the original distribution, α is the shape parameter of the Weibull distribution, β is the scale parameter of the Weibull distribution and X is the mean of the original distribution.

2.2. Analytical Fatigue Model

In the current analytical model, instead of comparing the applied stress to the residual strength of the ply, the first ply failure theory is used to determine if there is a failure in the structure due to the degradation of the residual strength. Four first ply failure theories, namely Tsai-Hill, Tsai-Wu, Hashin and Puck were individually combined with the Kassapoglou method and their accuracy is compared to the results from experiments and the original Kassapoglou method [25] for different stress ratios in Figure 2. A $[[\pm 45/0_2]_2]_s$ T800/5245 bismaleimide (BMI) laminate is used for the comparison. Table 1 shows the strength allowables as well as the mean and the standard deviation of the material used. Results show that the degradation model combined with all the failure theories is conservative with respect to the experimental results. Keeping

in mind the accuracy along with the ease of implementation, Tsai-Wu is chosen as the most suitable failure theory to predict the fatigue life. However, it is understood that the Tsai-Wu failure criterion does not always match test results, especially under biaxial compression, but it gives a good indication of first ply failure for other loading situations. Furthermore, the approach presented here can easily be modified to include a different failure criterion as necessary.

Table 1: Material properties of T800/5245 ply [33].

Property	**E1** (GPa)	**E2** (GPa)	**G12** (GPa)	ν_{12} (-)	X_t (MPa)	X_c (MPa)	Y_t (MPa)	Y_c (MPa)	**S** (MPa)
Mean	147	10.3	7	0.27	3460	1730	50	165	75
Standard Deviation					318.32	171.27	4.60	16.34	7.43

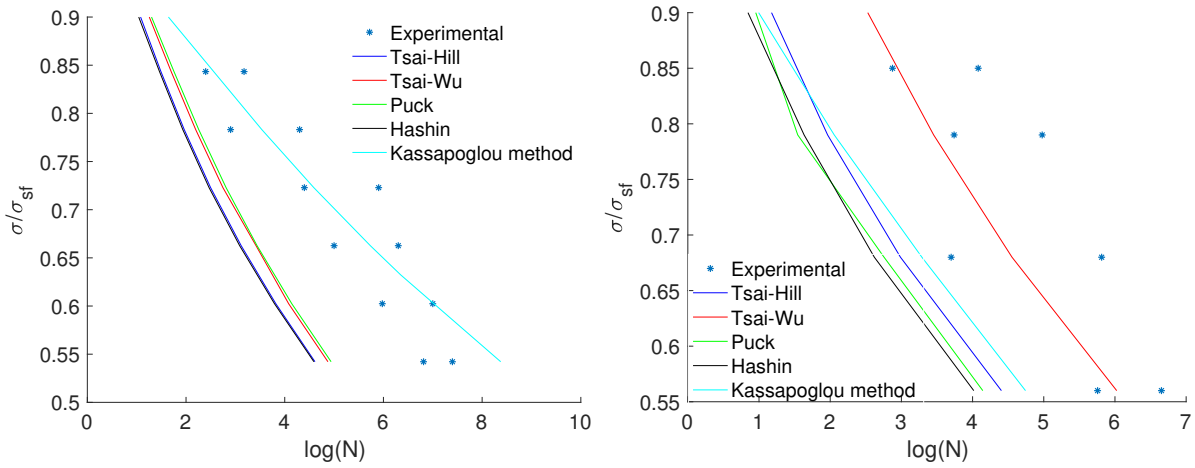

(a) R=0.1 **(b) R=10**

Figure 2: Comparison of 4 failure theories with results from the experimental and the original Kassapoglou model [25].

For the current analytical model, an assumption is made that the initial static strength follows a two parameter Weibull distribution. This assumption can be justified by the fact that the fatigue life of a composite material generally follows a two parameter Weibull distribution [34] [35] [36]. Since the Equation (2) describing the degradation of the residual strength is linear, both the residual strength and the initial static strength will also follow a two parameter Weibull distribution.

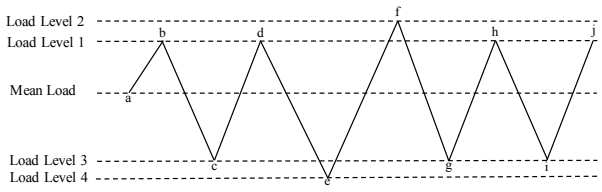

Figure 3: Simple spectrum with 4 load levels.

To predict failure under the spectrum loading, let us assume that the residual strength has a two parameter Weibull distribution with scale parameter α_{int} and a shape parameter β_{int} obtained by fitting a Weibull distribution to the stochastic static strength data. A simple spectrum loading comprising of peaks and valleys at different load levels is shown in Figure 3. At peak points in the spectrum, the stress ratio is obtained by taking into account the stress applied at the valley before the peak with stress applied at the peak. During the first cycle, the load increases to point a in the spectrum. As this is assumed to have stress ratio $R = 0$, no modification of R is necessary according to Equations (3) and (4). When the load reaches point a, residual strength and the Weibull parameters are degraded following steps 1-4 and the Tsai-Wu failure criterion is evaluated. If there is no failure, then, the load excursion from point a to point b is applied. At point b, the R value is calculated by using the stress values at a and b. If $R \neq 0$, the current Weibull parameters are modified using Equations (3) and (4). Then, the process of updating the residual strength and Weibull parameters is repeated and the Tsai-Wu failure criterion is evaluated again. For the load excursion from b to c, it is assumed again that c corresponds to $R = 0$. From this point on, and as long as the Tsai-Wu criterion does not indicate failure, the process is repeated following the steps described above.

With composite materials, there is a high scatter in fatigue life due to anisotropic heterogeneous characteristics, such as lay-up, manufacturing defects and imperfections, test complications, and environment [37]. To account for scatter in the calculation of the fatigue life, the B-basis reliability is used. The definition of a B value is that at least 90% of the population of values is expected to be equal to or exceed a particular property with confidence of 95%. Over a wide variety of tests on different carbon/epoxy materials, it has been found than on an S-N diagram, the reduction corresponding to the difference between B-Basis and mean life is approximately 20% on stress (vertically) [37, 38]. Thus in the analytical model, the calculated fatigue life is knocked down by 20%, to incorporate the effects of scatter. It should be noted that this 20% knockdown is an approximation and, given enough data, more accurate estimates of the B-Basis life can be obtained.

2.2.1. Verification

The analytical fatigue model is validated for spectrum loading by comparing it to the test results from the Glass/Epoxy laminate for the Wisper Spectrum [28] and the New Wisper Spectrum [29]. The experimental data was obtained from the OPTIMAT BLADES project [30] in which an extensive experimental campaign on a Glass/Epoxy material used in the Wind Turbine Rotor Blades industry was performed. Two types of lay up were considered in the tests; a unidirectional (UD) layup $[0_4]$ and a multidirectional (MD)

$[\pm 45/0]_4/\pm 45]$ lay-up. To calculate the Weibull distribution parameters for the initial static strength of the ply, data corresponding to R03 coupon from the OPTIMAT database [30] is used. Outliers from this datasets are removed and Maximum Likelihood Estimation (MLE) method is used to estimate the shape and the scale parameter. Table 2 shows the static strength allowables of the ply along with their shape and scale parameters.

Table 2: Properties of Glass/Epoxy laminate used in OPTIMAT project [30].

Laminate	**Property**	**E1** (GPa)	**E2** (GPa)	**G12** (GPa)	ν_{12} (-)	X_t (MPa)	X_c (MPa)	Y_t (MPa)	Y_c (MPa)	**S** (MPa)
UD	Mean	41.5	15	8.6	0.36	802	509	55	161	53
	Scale					854	532.81	56.34	165.62	80.61
	Shape					10.12	11.02	21.75	22.56	23.56

Figure 4 compares the fatigue life of the UD ply predicted by the analytical model to the experimental results for the single stress ratio as well as the spectrum load. There is a reasonable agreement observed between the analytical model and the experimental results for all the cases except for the stress ratio of 10, where the prediction of the analytical model is a bit on the conservative side. This discrepancy is expected given the fact that under compression, several failure modes such as micro-buckling, matrix local yielding and shear failure may compete and interact. This interaction of failure modes is not accounted for in the model as formulated.

The MD laminate consists of ±45 non-woven glass roving lamina and 0 degree UD ply. As there is not much information available on the ±45 non-woven glass roving, the ±45 lamina is represented by 2 UD plies; one oriented at 45 degrees and the other at -45 degrees, each having half the thickness of the ±45 lamina. In the Table 3, the static strength of the MD laminate modelled with only UD plies and calculated using the Tsai-Wu failure criterion is compared with the actual strength values obtained from the OPTIMAT database. As can be seen, the Tsai-Wu values are quite conservative because the analysis is done using First Ply Failure (FPF) methodology.

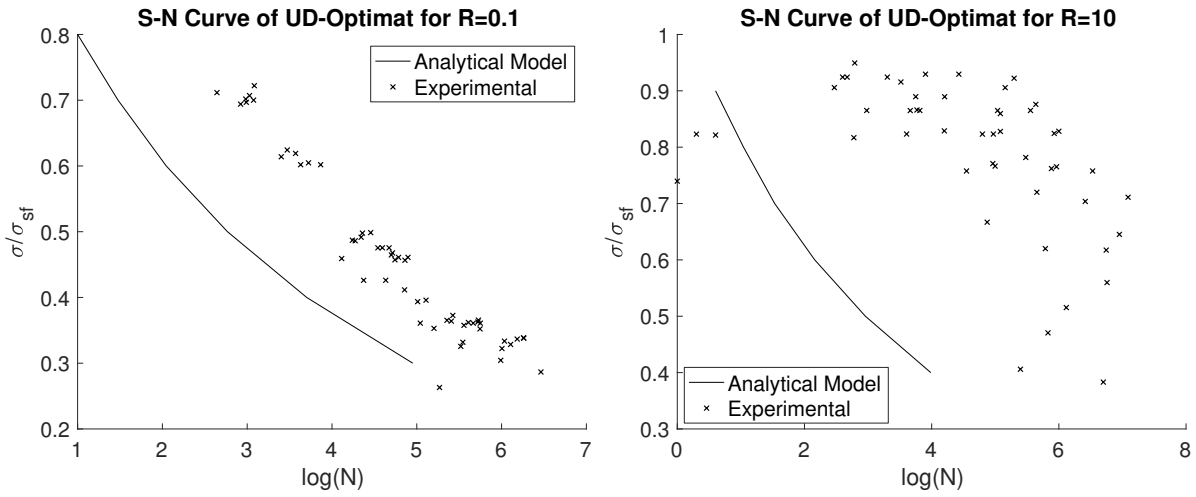

(a) R=0.1

(b) R=10

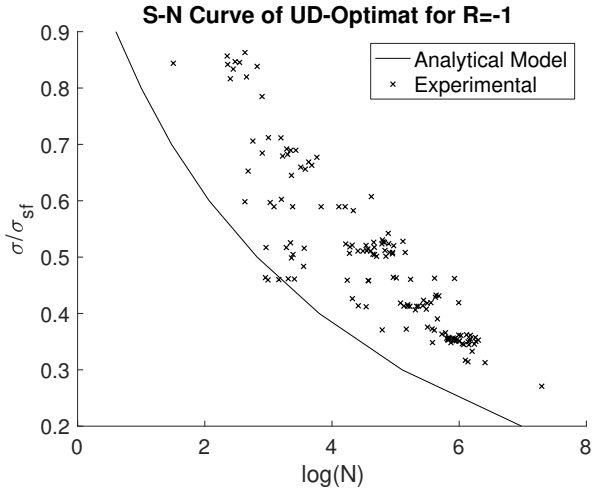

(c) R=-1

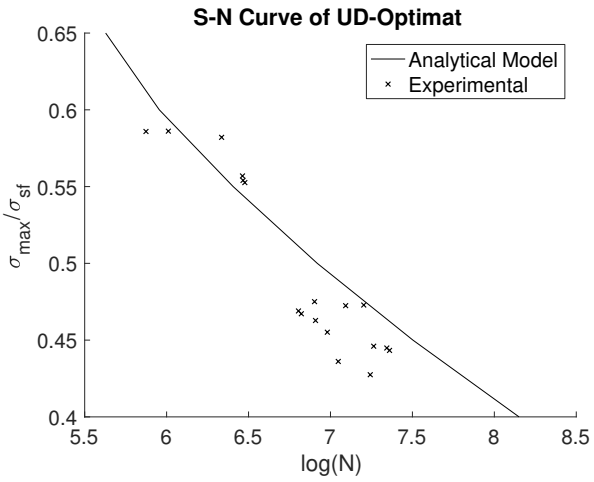

(d) Wisper Spectrum

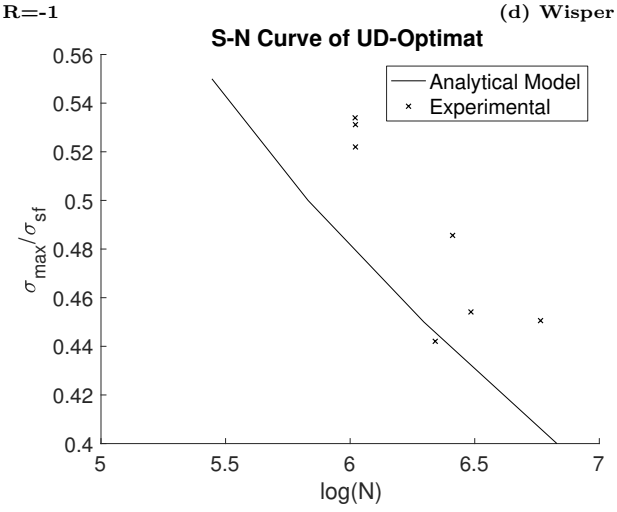

(e) New Wisper Spectrum

Figure 4: Comparison of fatigue life predicted by analytical model and experimental results for the UD laminate.

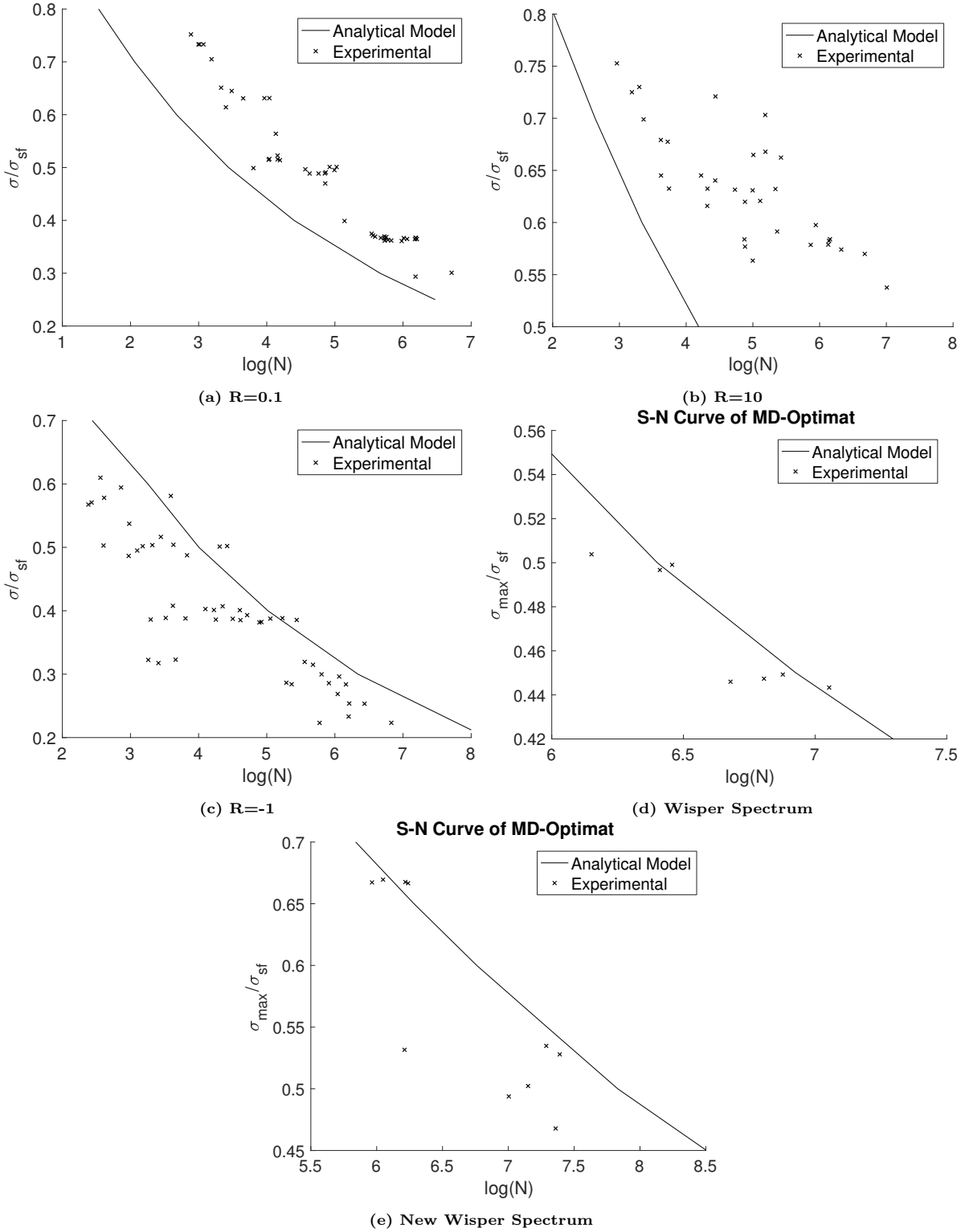

(a) R=0.1

(b) R=10

(c) R=-1

(d) Wisper Spectrum

(e) New Wisper Spectrum

Figure 5: Comparison of fatigue life predicted by analytical model and experimental results for the MD laminate.

The ±45 plies fail at a lower stress level compared to the 0 plies and as a result, the static strength values are quite conservative. In reality, the MD laminate will carry considerable load after the failure of ±45 plies. The static strength of the laminate then has to be predicted using progressive failure models with Ultimate Laminate Failure (ULF) failure criteria. To model the progressive failure of a laminate, a Stiffness Degradation Method (SDM) is formulated. In SDM, the damaged plies after the initial failure are modeled by reduced stiffnesses. Since Tsai-Wu is an interactive theory, there is no information on the mode of failure. Thus to use Tsai-Wu in SDM methodology, an assumption is made that if the stresses in the longitudinal direction are the main contributor to the failure index, then fiber has failed otherwise the matrix has failed [39].

For the current MD laminate, failure in the ±45 plies is matrix dominated and hence the transverse and the shear stiffness moduli are degraded as follows

$$E_{22_{new}} = D_1 E_{22} \tag{5}$$

$$G_{12_{new}} = D_2 G_{12} \tag{6}$$

The value of the degradation factors D_1 and D_2 is obtained by performing an optimization with an objective function of reducing the sum of two errors: the first error is between the stress-strain curve predicted using the SDM model and the experimental stress-strain data available in the OPTIMAT database and the second error is between the ultimate tensile strength predicted by the SDM model and the experiments. This multi-objective optimization results in 0.88 and 0.97 as the values for D_1 and D_2 respectively. As can be seen in Table 3, the SDM model gives a better estimate of the static strength in tension for the MD laminate. The static strength for compression still shows a significant difference and the main reason for that is the modelling of the ±45 plies in the laminate. The non-woven glass roving has a higher compressive strength compared to the combination of UD plies and hence the difference in the static strength values.

Table 3: Static strength allowables of the MD laminate.

Parameter	**Experimental Data**	**Tsai-Wu** FPF	**Tsai-Wu** SDM	**Units**
σ_t^{ult}	532	184	473	MPa
σ_c^{ult}	458	262	262	MPa

Figure 5 compares the fatigue life predictions by the analytical model using the SDM methodology to the experimental results for the MD laminate. For stress ratio of 0.1 and 10, there is a quite a good agreement on the fatigue life with the experimental results. For the stress ratio of -1 and the spectrum loading, even

though the predictions are slightly nonconservative, it is a good match as the analytical prediction can be considered to be within the scatter of the fatigue data.

Even though the comparisons to test results shown here are for glass/epoxy laminates having standard ply angles, the analytical fatigue model is still valid for carbon/epoxy specimens as well as non standard fiber orientations. Comparisons with carbon/epoxy laminates, showing good to excellent agreement with predictions, can be found in [25]. In addition, it should be emphasized that the analytical model is based on two quantities: The probability p that the strength of a given specimen is less than the applied cyclic stress at a given number of cycles and the residual strength which evolves with cycles. Of the two, the probability p is defined by the creation and evolution of damage during cycling. Therefore, any differences in the type of damage and its progress, arising due to the difference in the material or the orientation of the fiber are accounted for by the calculation of p as a function of cycles.

2.3. Assumptions in Analytical Fatigue Model

The process to predict failure by analyzing each step of a spectrum load until the laminate fails can become computationally expensive. For example, on an Intel i5 2.7 GHz single core processor, it took 3 hours to analyze the UD ply for the New Wisper spectrum with the maximum applied stress of 0.5 times the static failure stress. If an entire wing needs to be analyzed, the computational time would be in the range of 100 hours, which becomes quite expensive for an optimization process. Hence 3 assumptions have been made which can decrease the computational time quite significantly. In this section, the first 2 assumptions are discussed and the 3rd assumption will be explained later in the paper. To understand the basis of the first 2 assumptions, consider a simple spectrum shown in Figure 3.

The first assumption is that the ratio of degradation remains constant for a given load cycle. Looking at the Figure 3, the second load cycle consisting of points c and d, is similar to the 4th and the 5th load cycle consisting of points g, h, i and j respectively. Instead of repeating the analysis at the individual points, the model parameters can directly be degraded using the ratio calculated at the first instance. For example, the residual strength, if the combination of c and d repeats, n times is given by

$$\sigma_{r_2} = \sigma_{r_1} d_!^n \tag{7}$$

where σ_{r_1} is the residual strength before the first point of the load cycle, σ_{r_2} is the residual strength after the n similar load cycles and d_1 is the residual strength degradation ratio calculated during the first instance of the particular load cycle. Thus, for the 4th and the 5th load cycle, the degradation ratio can be applied directly to the residual strength and the Weibull distribution parameters.

A spectrum loading generally consist of a block of cycles which are repeated multiple times. The second assumption is then the extension of the first assumption over the entire block of the cycles. The ratio of degradation remains constant over the entire block. To explain the second assumption, consider a spectrum load made up by repeating the block of cycles described in Figure 3 seven times. To calculate the fatigue life over the entire spectrum, the degradation in different parameters is calculated by

$$x_2 = x_1 d_2^n \tag{8}$$

where x_1 is the value of the parameter at the start of the block, x_2 is the value of the parameter after the block is repeated n times (end of the spectrum) and d_2 is the degradation ratio of the parameter calculated during the first sequence of the block.

The second assumption can become nonconservative, as the ratio of the degradation increases with the decrease in the residual strength. Thus to be on the conservative side, the entire block of the cycles needs to be analyzed and the ratio of the degradation needs to be updated again after every 3rd sequence. With this approach the fatigue life for the spectrum load made up by repeating the block of cycles described in Figure 3 seven times is determined first by analyzing the first sequence of the block and calculating the degradation ratio for different parameters. Then the effect of the second and third sequence is directly calculated by degrading the model parameters by their respective ratios calculated for the first sequence. The degradation ratio is updated by analyzing the fourth sequence of the block and is then used to degrade the properties for the fifth and the sixth sequence and finally the seventh sequence is analyzed. Thus, the entire block of cycles is analyzed only three times instead of seven times resulting in a reduced computational effort.

Table 4 compares the residual strength after the application of the New Wisper spectrum on the UD laminate obtained from the full analysis and the analysis with the assumptions included. The maximum applied stress is 0.5 times the static failure stress. The second column lists the maximum change in the residual strength, and the third column shows the difference in the computational time required to perform the analysis. As can be seen, by implementing both the first and the second assumption, there is a good agreement with the original model with the error being less than 1%. With the use of these assumptions, the analytical model becomes faster by 92%.

2.4. Modification for Lamination Parameter Space

Typically a composite laminate is described by the ply angles and the stacking sequence. An alternative way to represent the composite laminate is through the use of lamination parameters. The lamination parameters describe the in-plane and out-of-plane behavior of the composite laminates and were first intro-

Table 4: Validity of the assumptions made to predict the fatigue life.

Assumption Type	ΔX (%)	Δt (%)
1	0.0013	85.2
2	0.92	56.4
Both 1 and 2	0.97	92.8

duced by Tsai and Pagano [40]. In an optimization process, the use of lamination parameters is advantageous as compared to the use of ply angles and stacking sequence. The first advantage is that a fixed number of lamination parameters describe the entire laminate irrespective of the number of plies, thus reducing the number of design variables. The second advantage is that as the lamination parameters are continuous, a gradient-based optimizer can be used, making the optimization process more efficient. For the current aeroelastic optimization process, lamination parameters are used to represent the composite laminate.

With the current fatigue model, only the laminates described by ply angles and stacking sequence can be analyzed. With the lamination parameters, there is no information on the number of the plies or the angle of the plies. As a result, the fatigue model is modified such that it can be applied to the lamination parameter domain.

From hereon, the analytical model to predict failure in the laminate described by ply angle and stacking sequence will be called the original model. To determine if the laminate has failed, the Tsai-Wu failure criterion has been implemented in the original model. The failure criterion in its original form explicitly depends on the ply angles and the stacking sequence. To adapt it for the lamination parameters, Ijsselmuiden et al. [41] formulated a failure envelope based on the conservative approximation of the Tsai-Wu failure criterion that does not explicitly depend on the ply angle. The approach assumes that all ply angles could be present at any location through the thickness of the laminate and thus is safe regardless of the ply angle. Khani et al. [42] modified the failure envelope such that it can be used with principal strains. In the current fatigue model, for the failure criterion, this modified Tsai-Wu failure envelope is implemented.

As the failure envelope works with the principal strains, the fatigue model is modified to work on principal strains rather than lamina stresses. Figure 6 depicts the flowchart of the fatigue model to determine failure for a composite defined by the lamination parameters. To determine the probability of failure, which is needed for calculating cycles to failure N, instead of comparing the lamina stresses in each ply to their residual strength, the value of the modified Tsai-Wu criterion of the entire laminate is compared to the failure index, which at the start is equal to 1. For this purpose, the Weibull distribution parameters of the Tsai-Wu criterion need to be calculated. Based on the statistical distribution of the static strength allowables,

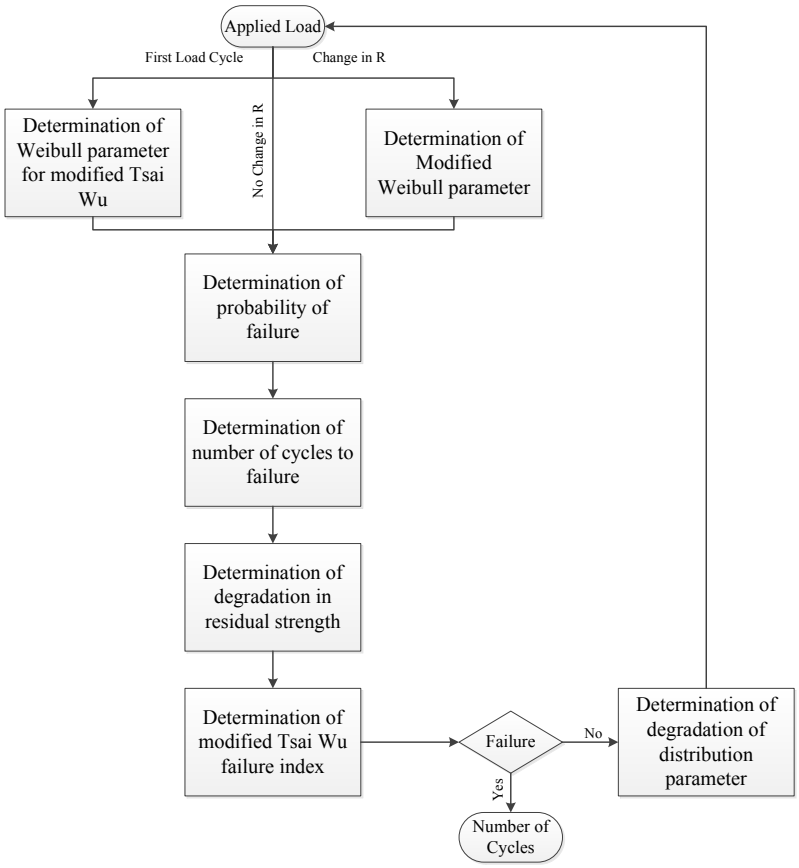

Figure 6: Algorithm for the modified fatigue model.

100,000 set of inputs to the Tsai-Wu failure criterion are randomly generated. A deterministic computation of the failure criterion on the randomly generated input is performed and the Weibull distribution of the modified Tsai-Wu is estimated. Figure 7 shows an example of the histogram generated by calculating the modified Tsai-Wu failure index for a set of 100,000 random input variables.

In the original model, the degradation in the residual strength of the ply is calculated with the Equation (2). In the case of the modified model, the stress terms in the equation are replaced by principal strains. The equation for the degradation in residual strength can then be expressed as

$$\begin{aligned} \sigma_r &= \sigma_{sf}(1-(1-\frac{\epsilon_i}{\epsilon_{sf}})\frac{n}{N-1} \\ \epsilon_r &= \epsilon_{sf}(1-(1-\frac{\epsilon_i}{\epsilon_{sf}})\frac{n}{N-1} \end{aligned} \tag{9}$$

where ϵ_i represents the principal strain of the laminate based on the applied stress and ϵ_{sf} represents

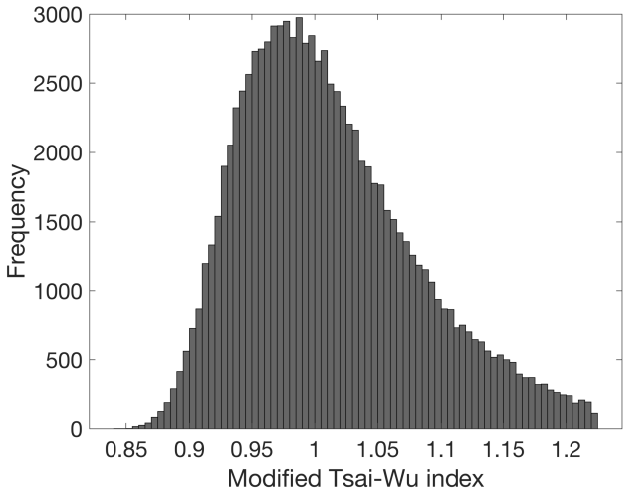

Figure 7: Histogram of the modified Tsai-Wu failure index generated using 100,000 sets of random input.

the principal strain at which the laminate will fail.

The distribution parameters of the modified Tsai-Wu criterion are degraded by R_{tw}, which is expressed as

$$R_{tw} = \frac{f}{f_r} \tag{10}$$

where f is the value of the modified Tsai-Wu criterion before the residual strength degradation and f_r is the value of the modified Tsai-Wu criterion after the residual strength degradation.

Figure 8 compares the result by the original model and the modified model for the OPTIMAT MD ply subjected to New Wisper spectrum. As expected, because of the conservative nature of the modified Tsai-Wu criterion [42], the fatigue predictions of the modified fatigue model are conservative compared to the original model.

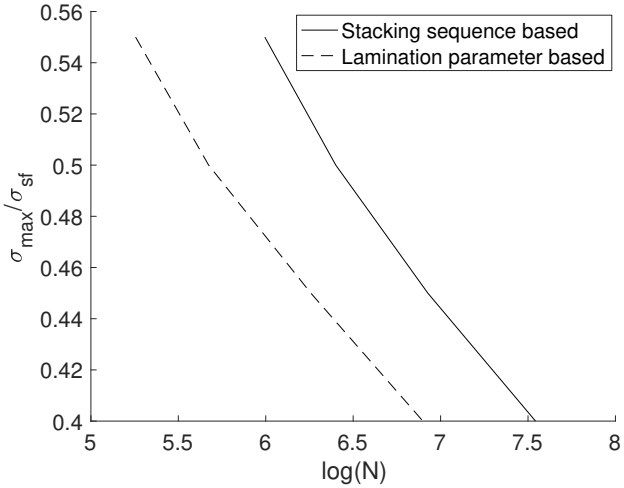

Figure 8: Comparing life prediction of model with lamination parameter and model with stacking sequence.

3. Optimization Studies

To understand the effect of including the proposed fatigue analysis over using the traditional knockdown factor in the design of the composite wing, the analytical fatigue model is integrated into PROTEUS [43], which is an in-house aeroelastic tool, developed at the Delft University of Technology, to carry out optimization of a composite wing. Figure 9 depicts the schematic representation of the framework of the PROTEUS. The process starts with discretizing the wing into multiple spanwise sections, where each section is defined by one or more laminates in the chord wise direction. Based on the laminate properties, a cross sectional modeller especially developed to deal with anisotropic shell cross-sections, uses the cross-sectional geometry to generate the Timoshenko stiffness matrices. A geometrically non linear aeroelastic analysis is carried out for multiple load cases by coupling the geometrically nonlinear Timoshenko beam model to an unsteady vortex lattice aerodynamic model. A linear dynamic aeroelastic analysis is carried out around the nonlinear static equilibrium solution. In the post processing, with the help of the cross sectional modeller, the strains in the three-dimensional wing structure are retrieved. The obtained strains are used to calculate the strength and buckling properties of the wing which are then fed to the optimizer as constraints. In the current study, fatigue properties of the wing (see the following section) will also be calculated using the analytical fatigue model and fed as a constraint to the optimizer. With respect to dynamic aeroelastic optimization, as the design changes during the optimization, the critical gust load cases also change [44]. As a result, at every design step, the critical load cases need to be identified. For this purpose, a Reduced Order Aeroelastic Model (ROAM) is used to identify critical gust load in a computationally efficient manner.

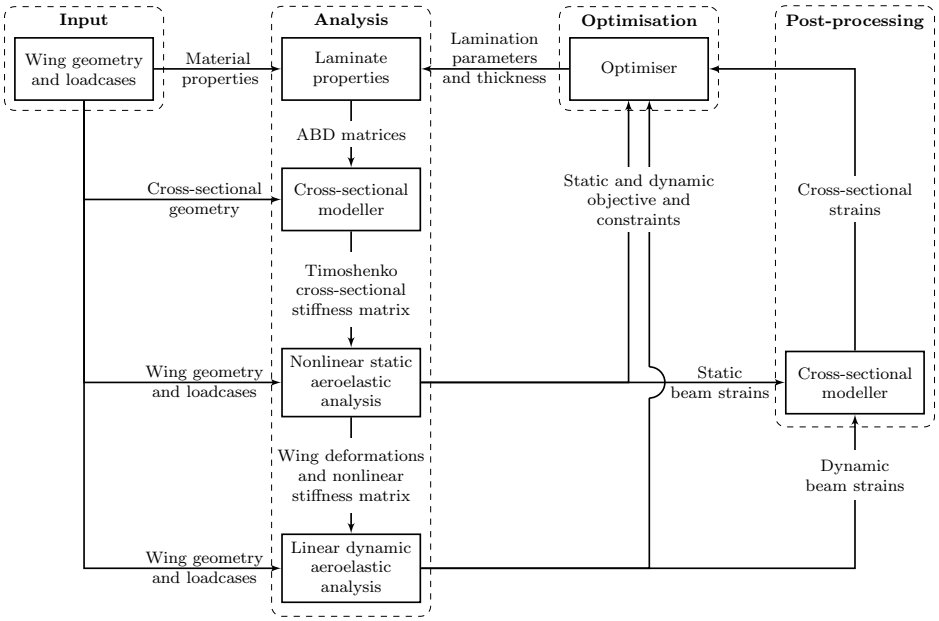

Figure 9: Framework of PROTEUS [43].

3.1. Fatigue Constraint

To analyze the wing for fatigue, a shortened version of the TWIST spectrum (Mini-TWIST) [45] is used as the load spectrum. The Mini-TWIST spectrum consists of ten flight levels where each flight level has ten different levels of stress ratio. The stress ratio has been normalized to the stress level at cruise condition. At each stress ratio, the number of cycles is different. The ten flight levels are repeated in a random manner to make a block of 4,000 flights which is equal to 58,442 cycles. This block is repeated 10 times, equivalent to 40,000 flights which is considered as the maximum life of the aircraft. A fatigue factor F is calculated for every laminate by subjecting it to Mini-TWIST spectrum for 10 times. F is defined as

$$F = r\frac{N_t}{N_f} \tag{11}$$

where r is the modified Tsai-Wu failure criterion at the time of failure, N_t represents the total cycles the structure has to withstand and N_f represents the total cycles to failure. If the laminate does not fail after the 40,000 flights, r is then the maximum modified Tsai-Wu failure criterion calculated in the spectrum.

For each laminate, running the fatigue model for 40,000 flights can become time consuming. Looking at the process to calculate the fatigue life in the lamination parameter domain, calculation of the Weibull parameters for different stress ratios is computationally the most expensive. In an effort to speed up the process, in addition to the 2 aforementioned assumptions discussed in section 2.3, a 3rd assumption is made. The ratio of change in the Weibull parameters for all the patches remains constant. The patch could be

design region or a laminate. Consider a wing consisting of 10 patches. The statistical distribution of the static strength of the material is described by Weibull parameters α_{int} and β_{int}. The wing is subjected to the Mini-TWIST spectrum. At the 2nd load step, the R ratio changes and hence Weibull distribution is modified as well. The new Weibull parameters $\alpha_{1_{new}}$ and $\beta_{1_{new}}$ for the first patch are calculated using the Equations (3) and (4) (it is recommended to use the most critical patch as determined by the highest value of the Tsai-Wu criterion). The modified Weibull parameters for rest of the patches are then calculated by

$$\begin{aligned} \alpha_{i_{new}} &= \alpha_{i_{int}} \frac{\alpha_{1_{new}}}{\alpha_{1_{int}}} \\ \beta_{i_{new}} &= \beta_{i_{int}} \frac{\beta_{1_{new}}}{\beta_{1_{int}}} \end{aligned} \tag{12}$$

where i is the patch number ranging from 2 to 10.

Thus, Weibull parameters at a new stress ratio are determined only for the single laminate and based on the ratio of change in the parameters, the Weibull parameters for all the other laminates are determined. Figure 10 depicts the delta plot of the percentage change in the residual strength value of the laminates with and without the 3rd assumption. The overall difference is less than 0.5%. The wing used is a CRM wing which is described in the next section. In terms of computational efficiency, without the 3rd assumption it takes 104 minutes to run a block of 4,000 flights and with the 3rd assumption, it takes 2 minutes. Thus, only with the 3rd assumption, 98% saving in the computational effort is achieved without sacrificing much in terms of accuracy.

3.2. Optimization approach

The NASA CRM [31], originally developed for the 4th AIAA drag prediction workshop, is used as a case study for the current analysis. The main characteristics of the CRM are summarized in Table 5. Figure 11 depicts the wing planform. Ribs, engine, leading edge devices and trailing edge devices are taken into account as concentrated masses. Stringers are also modelled to strengthen the top and bottom skin of the wing.

Two optimization studies are performed: one, an aeroelastic optimization without fatigue as a constraint, and two, an aeroelastic optimization with fatigue as a constraint. In the first one, a knockdown factor of 0.39 is applied to account for fatigue, damage and material scatter and a knockdown factor of 0.8 is applied to account for environment. Thus a net knockdown factor of 0.312 is applied to the stress allowables. In the second case, knockdown factors of 0.65 and 0.8 are applied to account for damage and environment respectively. Thus a net knockdown factor of 0.52 is applied to the stress allowables. Additionally, as was mentioned before, in the analytical model, the fatigue life is also reduced by 20% to account for fatigue

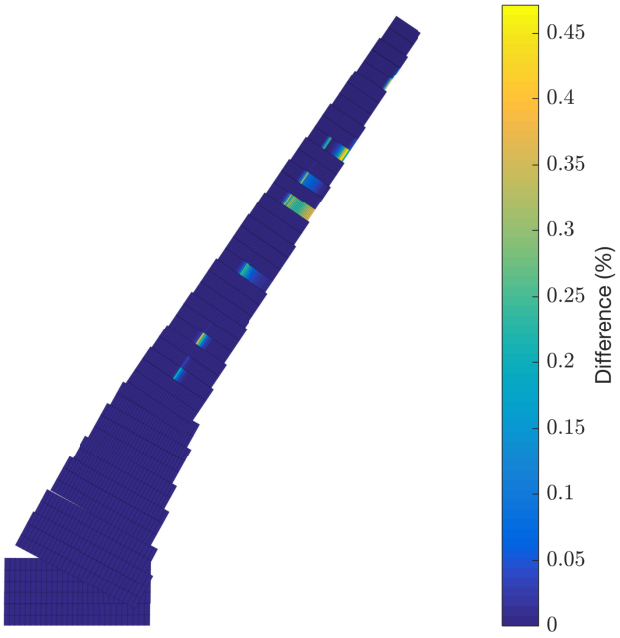

Figure 10: Delta plot of residual strength with and without 3rd assumption.

Table 5: Characteristics of the CRM wing.

Parameter	**Value**
Span	58.78 m
Leading edge sweep angle	35 deg
Wing aspect ratio	8.4
Taper ratio	0.28
Planform wing area	412 m^2
Cruise Mach	0.85
Design Range	14,300 km
Design Payload	45,000 kg
Maximum takeoff weight	296,000 kg

scatter. The UD AS4/8552 carbon/epoxy composite prepreg is used as the reference material. Table 6 shows the material properties along with the Weibull distribution parameters [46]. The optimization problem is shown in Table 7. The objective of the study is to minimize the structural weight of the wing. The wing is divided into 10 sections along the spanwise direction. For the top skin and the bottom skin, each spanwise section consists of two laminates in the chord-wise direction and for the spars, each spanwise section has only one laminate in the chord-wise direction. This results in 64 unique laminates. Laminates are symmetric and unbalanced. Every laminate is described by eight lamination parameters and one thickness variable, resulting in a total of 576 design variables. Figure 12 depicts the laminate distribution along the top skin of the wing. It also shows the stiffness for each laminate, where the wing stiffness distribution is represented

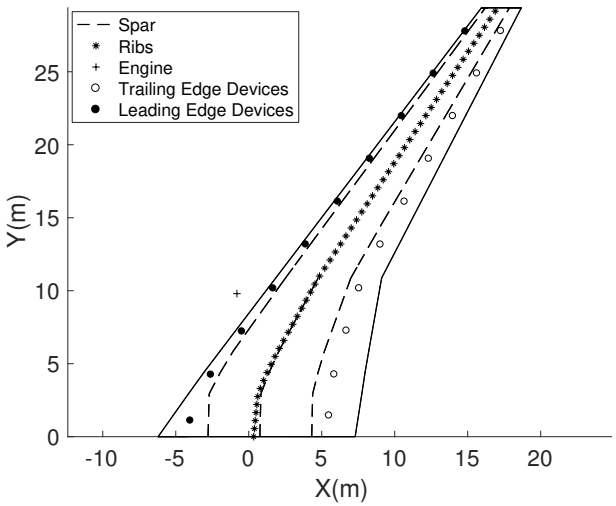

Figure 11: CRM wing planform and non structural mass distribution.

by the polar plot of thickness normalized modulus of elasticity $\hat{\mathbf{E}}_{11}(\theta)$ which is given by

$$\hat{\mathbf{E}}_{11}(\theta) = \frac{1}{\hat{\mathbf{A}}_{11}^{-1}(\theta)} \tag{13}$$

where $\hat{\mathbf{A}}$ is the thickness normalized membrane stiffness matrix and θ ranges from 0 to 360 degrees [47].

Table 6: Material Properties of AS4/8552.

Property	**Mean Value** (GPa)	**Scale** (GPa)	**Shape** (-)
E_{11}	128		
E_{22}	19.3		
G_{12}	4.8		
ν_{12}	0.3		
X_t	1.99	2.06	12.05
X_c	1.39	1.43	16.59
Y_t	0.064	0.067	11.12
Y_c	0.27	0.28	17.32
S	0.092	0.094	17.32

To ensure that lamination parameters represent a realistic ply distribution, feasibility equations formulated by Hammer et al. [48], Raju et al. [49] and Wu et al. [50] are applied. The aforementioned modified Tsai-Wu failure envelope is used to assess the static strength of the laminate. The stability of the panel in buckling is based on idealized buckling model formulated by Dillinger et al. [47]. To guarantee the static and dynamic aeroelastic stability of the wing, the real part of the eigenvalues of the state matrix should be less than zero at the flutter speed. For the optimization study with fatigue as a constraint, the analytical fatigue model is used to calculate the fatigue life of the laminate. The laminate should not fatigue during the

Table 7: Optimization Setup.

Type	Parameter	# parameters
Objective	Minimize Wing Mass	1
Design Variables	Lamination Parameter Laminate Thickness	576
Constraints	Laminate Feasibility	384
	Static Strength	1,024/load case
	Buckling	4,096/load case
	Fatigue	3,875
	Aeroelastic Stability	10/load case
	Local Angle of Attack	22/load case
	Total Constraints	4,259+5,152/load case

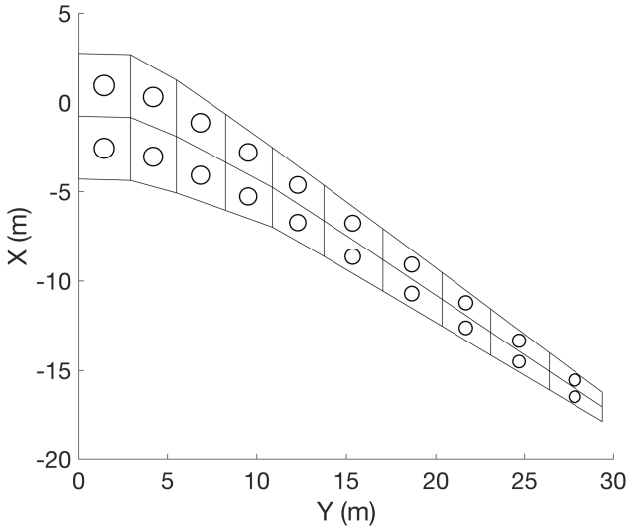

Figure 12: Laminate Distribution of the top skin of CRM.

design life of the aircraft which in the current case is assumed to be 40,000 flights with the aforementioned Mini-TWIST spectrum. The local angle of attack is constrained to a maximum of 12 degrees and a minimum of -12 degrees. For the current optimization, the Globally Convergent Method of Moving Asymptotes (GCMMA) developed by Svanberg [51] is used as a gradient-based optimizer.

Table 8 gives the information on the static load cases which are used for the current study. These load cases which were provided by NASA, represent the cruise condition, 2.5g symmetric pull up manoeuvre and -1g symmetric push down manoeuvre. With respect to dynamic load cases, 84 flight points covering the entire flight envelope are investigated. For each flight point, 40 gust gradients both positive as well as negative, ranging from 9 m to 107 m are considered. Figure 13 displays the flight envelope with their respective flight point ID. These load cases represent the limit load which is defined as the maximum load the wing expects in service. To satisfy the requirements for the ultimate load, an additional safety factor of

1.5 is applied to the strength and buckling values calculated for the limit loads.

Table 8: List of Loadcases.

Loadcase ID	V_{EAS} (m/s)	Altitude (m)	Load Factor (-)	Fuel level/Max fuel (%)
1	136	11,000	1	70
2	240	3,000	2.5	80
3	198	0	-1	80

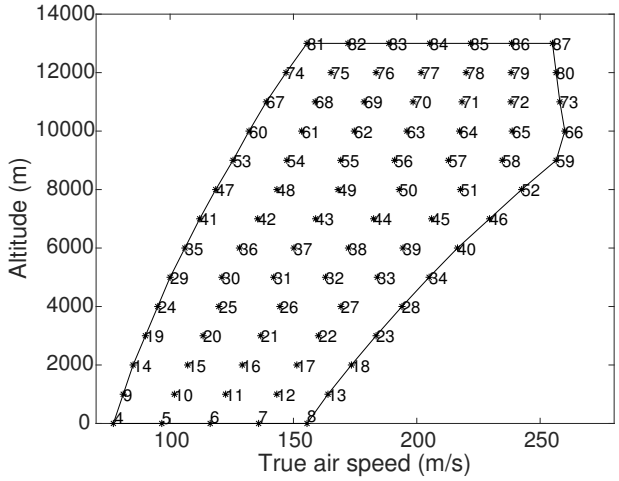

Figure 13: Flight Envelope.

3.3. Results

Figure 14 plots the critical constraints for both the optimization studies, one with and one without the analytical fatigue model. For the case of simplicity, from hereon, the case without the fatigue model will be referred to as the first study and the case with the fatigue model will be referred to as the second study. For the first study, the wing is critical in both strain and buckling. The inboard part of the top skin and spar is buckling critical whereas the outer part is critical in strain. The bottom skin is mainly driven by strain. In the case of the second study, similar trends can be observed. However, the wing is also critical in fatigue. The middle/outboard part of both top and bottom skins and the inboard part of the front spar are driven by fatigue.

Figure 15 shows the stiffness and the thickness distribution of the optimization studies. The stiffness distribution is represented by the polar plot of thickness normalized modulus of elasticity defined in Equation 13 where the wing axis constitutes the 0° direction. A circle as shown in Figure 12 represents a quasi isotropic laminate having equal stiffness in all direction whereas a deformed plot represents a tailored stiffness distribution. With respect to Figure 15, the region near the wing root is dominated by buckling and as

a result, the out of plane stiffness properties are more pronounced as compared to the rest of the wing in both the studies. With respect to middle and outboard part of the wing, for both the studies, the in plane stiffnesses in the top skin are oriented forward to increase the nose down twist and shift the load inboard. Figure 16 compares the twist distribution at 1g and 2.5g condition for wing optimized in the first and the second study. The middle part of the wing is critical in fatigue in the second study, resulting in a stiffness tailoring and thickness distribution which leads to a higher washout and hence reduced load compared to the wing in the first study. Looking at the in plane stiffness in the inboard part of the bottom skin, in the first study, the in plane stiffness shape is narrower than the second study, indicating more concentration of plies in 0 direction to increase the load carrying capacity as it has lower strength allowables because of the conservative knockdown factor.

Figure 17 compares the critical static and dynamic loads acting on the bottom skin of the optimized wing for both the studies. For each laminate, the number indicates the critical flight point and the colour indicates the critical gust gradient. The laminates with grey colour are critical with respect to the static load cases. Flight points 1, 2 and 3 are static load cases described in Table 8 and the rest are the dynamic flight points as shown in Figure 13. As can be seen, the middle part of the wing where fatigue is critical in the second study has different critical loads as compared to the wing in the first study. The wing optimized with fatigue model is more critical to static loads in the middle part whereas the wing optimized with conservative knockdown factor is more critical to dynamic loads in the middle part.

Looking at the thickness distribution, as expected, the optimized wings in the first study where a knockdown of 68% is applied to the material allowables, are thicker compared to the wings in the second study. The weight of the wing in the first study is 12,129 kg, whereas, in the second study, the wing weighs at 9,416 kg. Thus, by including analytical fatigue model, the weight of the wing can be reduced by approximately 22%. Additionally, the maximum fatigue factor for the wing in the first study is 0.75.

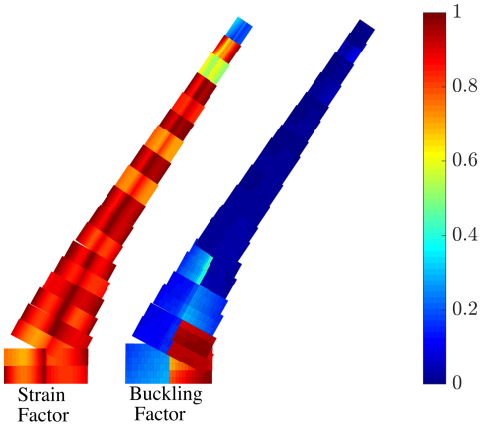

(a) Top Skin without fatigue model

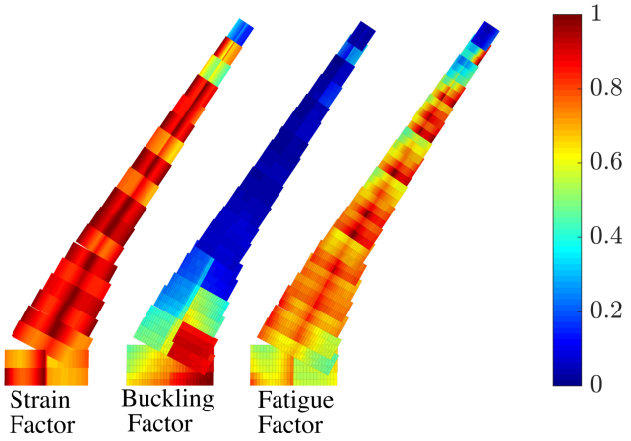

(b) Top Skin with fatigue model

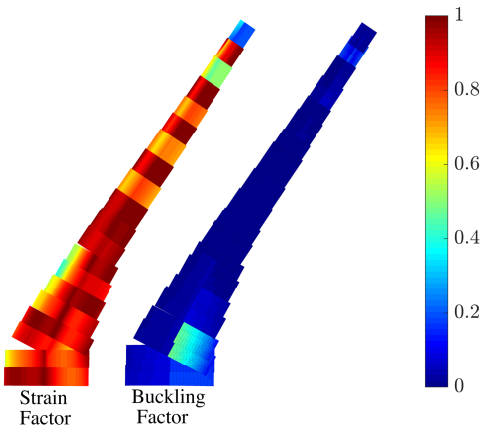

(c) Bottom Skin without fatigue model

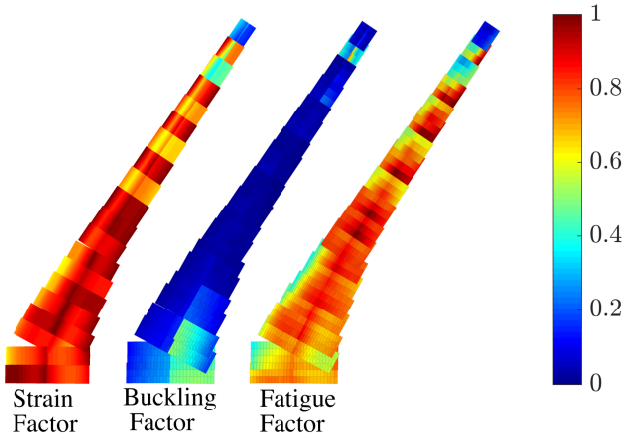

(d) Bottom Skin with fatigue model

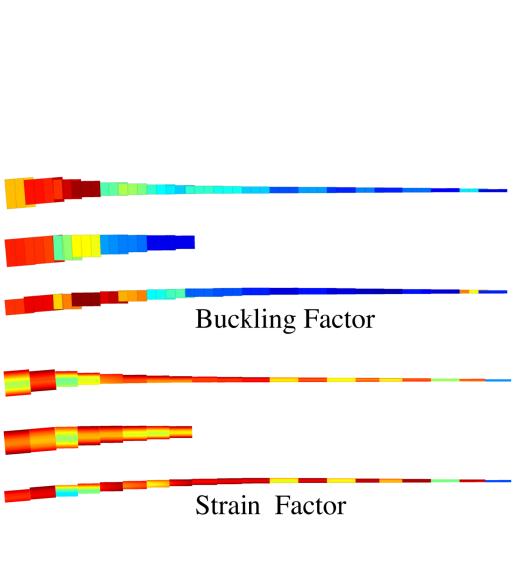

(e) Spars without fatigue model

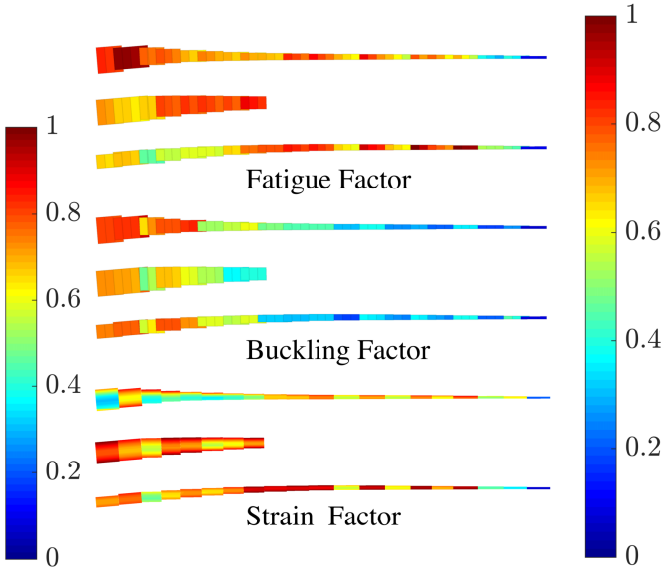

(f) Spars with fatigue model

Figure 14: Value of the critical constraints for the optimized CRM wing.

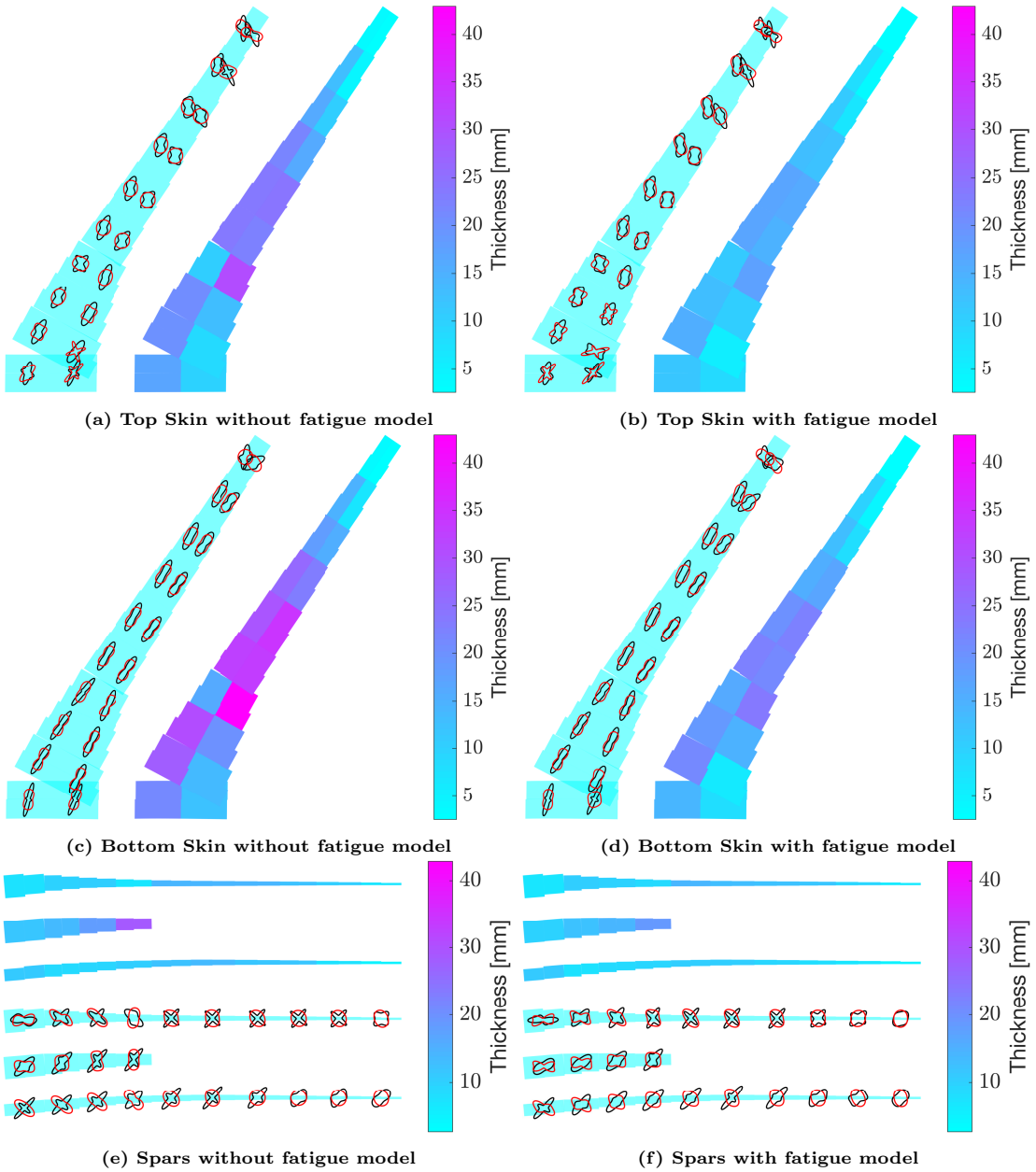

(a) Top Skin without fatigue model

(b) Top Skin with fatigue model

(c) Bottom Skin without fatigue model

(d) Bottom Skin with fatigue model

(e) Spars without fatigue model

(f) Spars with fatigue model

Figure 15: Stiffness and thickness distribution for the optimized CRM wing (In-plane stiffness: black, out-of-plane stiffness: red).

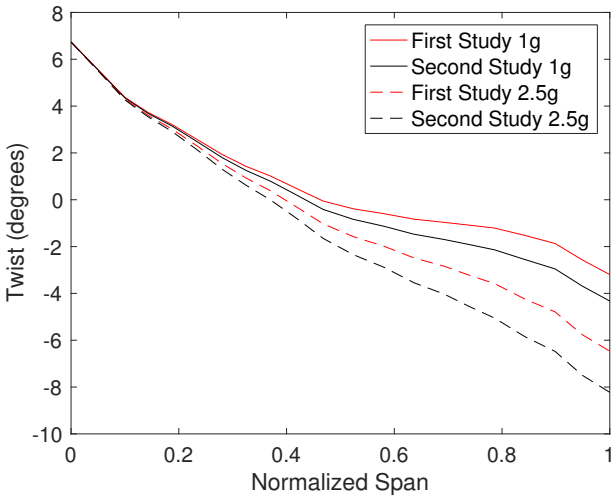

Figure 16: Total twist distribution for the CRM wing optimized in the first and the second study.

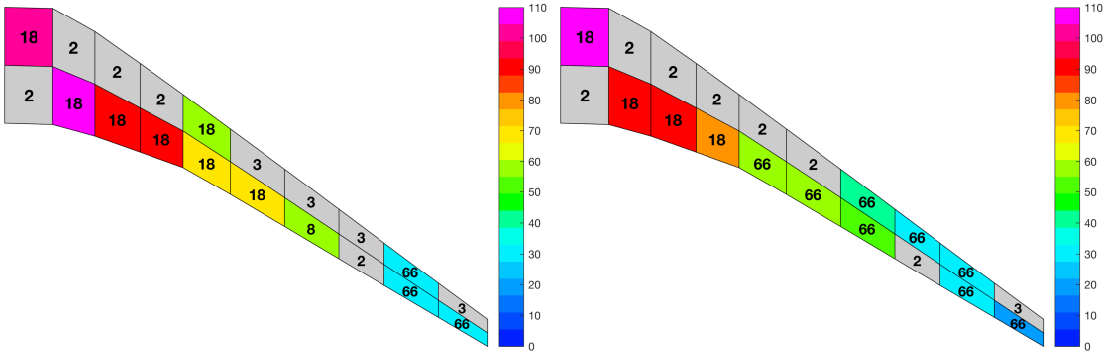

(a) Bottom Skin with fatigue model **(b) Bottom Skin without fatigue model**

Figure 17: Critical static and dynamic loads on the bottom skin of the optimized CRM wing

4. Conclusions

An aeroelastic optimization method including fatigue as a constraint for composite wings was formulated. Fatigue was accounted in the optimization using the analytical fatigue model. The analytical fatigue model is a residual strength degradation model based on the method developed by Kassapoglou.

Kassapoglou's method was extended by adding a first ply failure theory to determine the failure of the ply. Different first ply failure theories were compared to the experimental data and Tsai Wu was found to have the best mix of accuracy and ease of implementation. Furthermore, it was assumed that the initial strength distribution would follow a Weibull distribution. The predictions of the fatigue model were compared to the test results of UD and MD glass/epoxy laminate for the Wisper and the New Wisper spectrum. Reasonable agreements were found between the predicted and the experimental results, with the analytical model being conservative. Additionally, the analytical model was also extended to work with laminates described by lamination parameters instead of ply angles and stacking sequence. Since the failure criterion in the lamination parameter domain was conservative in nature, the life predictions were also conservative compared to the prediction for laminates defined by ply angles.

The developed analytical fatigue model was integrated into the aeroelastic and optimization tool PROTEUS. Two optimization studies of the CRM wing were carried out, one with fatigue as a constraint using the analytical fatigue model and another was the traditional one by using knockdown factors on material allowables to account for fatigue. To account for fatigue, the maximum design life of 40,000 flights based on Mini TWIST spectrum was assumed.

Results show that a composite wing is not only critical in strength and buckling but also in fatigue when accounted for explicitly rather than using the conservative knockdown factors which limit the fatigue loads to a small fraction of the limit load. The middle part of the wing is critical in fatigue and as a result, optimum stiffness and thickness distribution achieved lead to a higher washout and thus reduced the load in the middle part. The critical dynamic and static loads for the optimum configurations are also different when fatigue is accounted for by the analytical model. The middle part of the wing optimized with fatigue constraint is critical with respect to static loads whereas the middle part of the wing optimized with conservative knockdown factor is critical with respect to dynamic loads. Furthermore, by including a mathematical fatigue model instead of a conservative knockdown factor, the weight of the wing is reduced by 22%.

5. Acknowledgements

The authors are grateful to Dr. R. Nijssen for providing additional sources of test data from the OPTIMAT program.

References

[1] C. Jutte, B. K. Stanford, Aeroelastic tailoring of transport aircraft wings: State-of-the-art and potential enabling technologies, NASA Tech. Rep. TM2014-218252.

[2] N. Post, S. Case, J. Lesko, Modeling the variable amplitude fatigue of composite materials: A review and evaluation of the state of the art for spectrum loading, International Journal of Fatigue 30 (12) (2008) 2064–2086.

[3] J. Degrieck, W. Van Paepegem, Fatigue damage modeling of fibre-reinforced composite materials: Review, Applied Mechanics Reviews 54 (4) (2001) 279–300.

[4] V. Passipoularidis, P. Brøndsted, Fatigue evaluation algorithms: review, Tech. rep., Danmarks Tekniske Universitet, Risø Nationallaboratoriet for Bæredygtig Energi (2010).

[5] M. Miner, et al., Cumulative fatigue damage, Journal of applied mechanics 12 (3) (1945) A159–A164.

[6] W. V. Paepegem, J. Degrieck, P. D. Baets, Finite element approach for modelling fatigue damage in fibre-reinforced composite materials, Composites Part B: Engineering 32 (7) (2001) 575 – 588.

[7] H. Whitworth, A stiffness degradation model for composite laminates under fatigue loading, Composite structures 40 (2) (1997) 95–101.

[8] J. Brunbauer, G. Pinter, Fatigue life prediction of carbon fibre reinforced laminates by using cycle-dependent classical laminate theory, Composites Part B: Engineering 70 (2015) 167 – 174.

[9] T. Philippidis, V. Passipoularidis, Residual strength after fatigue in composites: Theory vs. experiment, International Journal of Fatigue 29 (12) (2007) 2104–2116.

[10] C. Dahlen, G. S. Springer, Delamination growth in composites under cyclic loads, Journal of Composite Materials 28 (8) (1994) 732–781.

[11] H. Bergmann, R. Prinz, Fatigue life estimation of graphite/epoxy laminates under consideration of delamination growth, International Journal for Numerical Methods in Engineering 27 (2) (1989) 323–341.

[12] L. J. Broutman, S. Sahu, A new theory to predict cumulative fatigue damage in fiberglass reinforced plastics, in: Composite materials: Testing and design (second conference), ASTM International, 1972.

[13] J. R. Schaff, B. D. Davidson, Life prediction methodology for composite structures. Part I - constant amplitude and two-stress level fatigue, Journal of composite materials 31 (2) (1997) 128–157.

[14] J. R. Schaff, B. D. Davidson, Life prediction methodology for composite structures. Part II - spectrum fatigue, Journal of composite materials 31 (2) (1997) 158–181.

[15] H. Hahn, R. Kim, Proof testing of composite materials, Journal of Composite Materials 9 (3) (1975) 297–311.

[16] Z. Hashin, Cumulative damage theory for composite materials: residual life and residual strength methods, Composites Science and Technology 23 (1) (1985) 1–19.

[17] P. C. Chou, R. Croman, Residual strength in fatigue based on the strength-life equal rank assumption, Journal of Composite Materials 12 (2) (1978) 177–194.

[18] J. N. Yang, Fatigue and residual strength degradation for graphite/epoxy composites under tension-compression cyclic loadings, Journal of Composite Materials 12 (1) (1978) 19–39.

[19] J. N. Yang, D. L. Jones, Statistical fatigue of graphite/epoxy angle-ply laminates in shear, Journal of Composite Materials 12 (4) (1978) 371–389.

[20] J. Yang, C. Sun, Proof test and fatigue of unnotched composite laminates, Journal of Composite Materials 14 (2) (1980) 168–176.

[21] J. Yang, S. Du, An exploratory study into the fatigue of composites under spectrum loading, Journal of Composite Materials 17 (6) (1983) 511–526.

[22] T. Adam, R. Dickson, C. Jones, H. Reiter, B. Harris, A power law fatigue damage model for fibre-reinforced plastic laminates, Proceedings of the Institution of Mechanical Engineers, Part C: Journal of Mechanical Engineering Science 200 (3) (1986) 155–166.

[23] J. A. Epaarachchi, P. D. Clausen, An empirical model for fatigue behavior prediction of glass fibre-reinforced plastic composites for various stress ratios and test frequencies, Composites Part A: Applied science and manufacturing 34 (4) (2003) 313–326.

[24] K. L. Reifsnider, W. Stinchcomb, A critical-element model of the residual strength and life of fatigue-loaded composite coupons, in: Composite Materials: Fatigue and Fracture, ASTM International, 1986.

[25] C. Kassapoglou, Fatigue life prediction of composite structures under constant amplitude loading, Journal of Composite Materials 41 (22) (2007) 2737–2754.

[26] C. Kassapoglou, Fatigue of composite materials under spectrum loading, Composites Part A: Applied Science and Manufacturing 41 (5) (2010) 663–669.

[27] C. Kassapoglou, Fatigue model for composites based on the cycle-by-cycle probability of failure: implications and applications, Journal of Composite Materials 45 (3) (2011) 261–277.

[28] A. Tenhave, Wisper and wisperx: Final definition of two standardised fatigue loading sequences for wind turbine blades, NASA STI/Recon Technical Report N 94.

[29] B. Bulder, J. Peeringa, D. Lekou, P. Vionis, F. Mouzakis, R. Nijssen, New wisper creating a new standard load sequence from modern wind turbine data. (2005).
URL `<http://www.kc-wmc.nl/optimatblades/ Publications>`

[30] Optimat blades material database (2006).
URL `< http://www.wmc.eu/optimatblades.php>`

[31] J. C. Vassberg, M. A. DeHaan, S. M. Rivers, R. A. Wahls, Development of a common research model for applied cfd validation studies, in: 26th AIAA Applied Aerodynamics Conference, Honolulu, Hawaii, 2008.

[32] C. Kassapoglou, Modeling the Effect of Damage in Composite Structures: Simplified Approaches, John Wiley & Sons, 2015, Ch. 6.
[33] N. Gathercole, H. Reiter, T. Adam, B. Harris, Life prediction for fatigue of t800/5245 carbon-fibre composites: I. constant-amplitude loading, International Journal of Fatigue 16 (8) (1994) 523–532.
[34] W. Hwang, K. Han, Statistical study of strength and fatigue life of composite materials, Composites 18 (1) (1987) 47–53.
[35] J. N. Yang, Fatigue and residual strength degradation for graphite/epoxy composites under tension-compression cyclic loadings, Journal of Composite Materials 12 (1) (1978) 19–39.
[36] W. Yao, N. Himmel, Statistical analysis of data from truncated fatigue life and corresponding residual strength experiments for polymer matrix composites, International journal of fatigue 21 (6) (1999) 581–585.
[37] J. Tomblin, W. Seneviratne, Determining the fatigue life of composite aircraft structures using life and load-enhancement factors, Final report, Air Traffic Organization, Washington DC, USA.
[38] R. Whitehead, H. Kan, R. Cordero, E. Saether, Certification testing methodology for composite structures, Volumes I and II, Report No. NADC-87042-60 (DOT/FAA/CT-86-39).
[39] K.-S. Liu, S. W. Tsai, A progressive quadratic failure criterion for a laminate, Composites Science and Technology 58 (7) (1998) 1023–1032.
[40] S. Tsai, N. Pagano, Invariant Properties of Composite Materials, in: Composite Materials Workshop, Technomic Publishing Co., Westport, 1968, pp. 233–253.
[41] S. T. Ijsselmuiden, M. M. Abdalla, Z. Gurdal, Implementation of strength-based failure criteria in the lamination parameter design space, AIAA journal 46 (7) (2008) 1826.
[42] A. Khani, S. T. IJsselmuiden, M. M. Abdalla, Z. Gürdal, Design of variable stiffness panels for maximum strength using lamination parameters, Composites Part B: Engineering 42 (3) (2011) 546–552.
[43] N. P. M. Werter, R. De Breuker, A novel dynamic aeroelastic framework for aeroelastic tailoring and structural optimisation, Composite Structures 158 (2016) 369–386. doi:10.1016/j.compstruct.2016.09.044.
[44] D. Rajpal, E. Gillebaart, R. D. Breuker, Preliminary aeroelastic design of composite wings subjected to critical gust loads, Aerospace Science and Technology 85 (2019) 96 – 112.
[45] H. Lowak, J. DeJonge, J. Franz, D. Schütz, Minitwist - a shortened version of twist, NLR MP 79018 U.
[46] E. Clarkson, Hexcel 8552 AS4 unidirectional statistical analysis report.
[47] J. Dillinger, T. Klimmek, M. M. Abdalla, Z. Gürdal, Stiffness optimization of composite wings with aeroelastic constraints, Journal of Aircraft 50 (4) (2013) 1159–1168.
[48] V. B. Hammer, M. Bendsøe, R. Lipton, P. Pedersen, Parametrization in laminate design for optimal compliance, International Journal of Solids and Structures 34 (4) (1997) 415–434.
[49] G. Raju, Z. Wu, P. Weaver, On further developments of feasible region of lamination parameters for symmetric composite laminates, in: 55th AIAA/ASMe/ASCE/AHS/SC Structures, Structural Dynamics, and Materials Conference, 2014, p. 1374.
[50] Z. Wu, G. Raju, P. M. Weaver, Framework for the buckling optimization of variable-angle tow composite plates, AIAA Journal 53 (12) (2015) 3788–3804.
[51] K. Svanberg, A class of globally convergent optimization methods based on conservative convex separable approximations, SIAM journal on optimization 12 (2) (2002) 555–573.